JOURNAL OF SOLID STATE CHEMISTRY **131,** 38–42 (1997)
ARTICLE NO. SC977298

The Crystal Structure of $Cs_2TiSi_6O_{15}$

I. E. Grey,* R. S. Roth,† and M. L. Balmer‡

*CSIRO Division of Minerals, Melbourne, Australia; †National Institute of Standards and Technology, Gaithersburg, Maryland 20899; and ‡Battelle, Pacific Northwest National Laboratory, Richland, Washington 99352

Received October 24, 1996; accepted January 28, 1997

Crystals of a new titanosilicate phase, $Cs_2TiSi_6O_{15}$, were grown from a cesium vanadate flux. The compound has monoclinic symmetry, space group $C2/c$, with $a = 13.386(5)$, $b = 7.423(3)$, $c = 15.134(5)$ Å, $\beta = 107.71(3)°$, $Z = 4$. The crystal structure was solved using single crystal X-ray data (Mo$K\alpha$ radition) and refined to $R(F) = 0.039$ for 1874 unique reflections. In the structure, isolated titanium-centred octahedra and silica-centred tetrahedra share all corners to form an open framework structure containing large cavities in which the cesium ions are located. Each cavity is bound by three 5-rings, two 6-rings, and two 8-rings. The cavities are linked via the 8-rings into channels parallel to [101]. The cesium ions occur in pairs along the channels, separated by 3.765(2) Å.

INTRODUCTION

An important new development in inorganic microporous materials was the discovery in 1989 of a family of microporous titanosilicates, incorporating octahedrally coordinated Ti^{4+} ions (1, 2). The TiO_6 octahedra corner-link to SiO_4 tetrahedra to form the host framework. Members of the family have been commercially developed (Engelhard Corporation titanosilicates, ETS) for application as molecular sieves and selective catalysts (1). These compounds extended earlier developments in catalyst chemistry based on enhanced selective catalytic activity of microporous silicas by partial isomorphous replacement of tetrahedrally coordinated Si^{4+} by Ti^{4+} (3).

Further stimulus for research on the preparation and characterization of titanosilicates has come from the recognition that these compounds are effective ion exchangers for selective removal of cesium from radioactive, sodium-rich wastes (4). Recent work at Pacific Northwest National Laboratory has shown that certain Cs_2O–TiO_2–SiO_2 compositions can be thermally converted to crystalline titanosilicates with high durabilities toward leaching (5). One of the new compounds, with composition $CsTiSi_2O_{6.5}$, has a zeolitic structure closely related to that for pollucite, $CsAlSi_2O_6$ (6). Pollucite has been reported to be an excellent candidate for cesium containment (7). Whereas pollucite contains only tetrahedrally coordinated cations, the titanium derivative has 5-coordinated Ti^{4+} (6).

As part of a program on the characterization of $CsTiSi_2O_{6.5}$, single crystals were grown from a cesium vanadate flux. In addition to the desired compound, crystals were also obtained of another cesium titanosilicate with a higher silica content, $Cs_2TiSi_6O_{15}$. The X-ray diffraction data and unit cell dimensions for the second phase could not be reconciled with any known structure type. We report here the structural characterization of this phase.

EXPERIMENTAL

Synthesis and Characterization

A mixture of 0.08 g of microcrystalline $CsTiSi_2O_{6.5}$ and 0.07 g of $CsVO_3$ was sealed in a 3 mm diameter platinum tube. The tube was placed in a vertical tube furnace at 800°C. The temperature was increased to 1100°C at a heating rate of 50°C/h, held for 1 h at 1100°C, then cooled to 650°C at a rate of 1°C/h. Despite the tube being sealed the flux was found to have penetrated the walls of the tube and crystals were found both outside and inside the tube. After the flux was dissolved in warm water, crystals of four different phases were identified. Three of these were known phases, $CsTiSi_2O_{6.5}$, rutile, and cristobalite. The fourth and most prevalent phase comprised relatively large (0.1–0.5 mm), colorless, transparent tabular-shaped crystals showing high birefringence under a polarizing microscope.

Several of the crystals were examined by X-ray diffraction using the precession method. They were all found to be single crystals having C-centered monoclinic symmetry, with approximate cell dimensions $a = 13.4$, $b = 7.4$, $c = 15.1$ Å, $\beta = 108°$. The dominant faces of the plate-like crystals were found to be $\{001\}$. Systematic absences in the precession photos were consistent with the space groups $C2/c$ and Cc.

Wavelength dispersion electron microprobe analyses were made on sectioned and polished crystals using a JEOL Model JXA-8900R Superprobe operated at 15 kV and 20 nA. Standards used were synthetic pollucite, $CaAlSi_2O_6$, rutile, and vanadium metal. The analyses showed small

0022-4596/97 $25.00

variations within and between crystals. The ranges obtained were 36.0–37.4 wt% Cs, 22.5–23.3 wt% Si, 7.2–8.7 wt% Ti, and 0.5–0.6 wt% V.

Data Collection and Structure Analysis

For the data collection, a tabular crystal was mounted along *b* on a Siemens AED diffractometer employing Mo$K\alpha$ radiation. Lattice parameters were determined by the least-squares technique applied to the setting angles of reflections with $11 < \theta < 26^\circ$. Intensities were collected using θ–2θ scans. Three standard reflections which were monitored every 50 reflections to correct for intensity drift showed no significant deviations. Details of the data collection, data processing and structure refinement are given in Table 1.

Working in the centrosymmetric space group $C2/c$, the positions of a cesium and a titanium atom were obtained from an analysis of the three dimensional Patterson map. The silicon and oxygen atoms were located in successive Fourier and difference Fourier maps. Refinement of all coordinates, isotropic displacement parameters and an extinction parameter converged at a high $R(F)$ value of 0.15. Release of anisotropic displacement parameters resulted in a rapid convergence to $R(F) = 0.039$ for all 1874 independent reflections. The refinement was based on F^2 and the final w$R(F^2)$ was 0.13. Some of the oxygen atoms had large anisotropic displacement parameters. Attempts to model these with split atoms and with refinements in Cc gave no further improvement in the R values. The highest peaks in the difference Fourier map obtained after the final refinement were 1.2 and 1.4 $e/Å^3$, close to the cesium atoms.

The data processing, including the absorption correction, was made using SHELX-76 (8) and the structure refinement was carried out with SHELXL93 (9).

TABLE 1
Details of X-Ray Data Collection and Refinement

Formula mass	721.7
Space group	$C2/c$
a, Å	13.386(5)
b, Å	7.423(3)
c, Å	15.134(5)
β, deg.	107.71(3)
V, Å^3	1432.5
Z	4
Radiation	Mo$K\alpha$, $\lambda = 0.7107$ Å
Linear absorption ocefficient, mm^{-1}	6.30
Absorption correction	Analytical, using crystal faces (Ref. 8)
Transmission factors	0.244 to 0.551
Calculated density, Mg m^{-3}	3.35
Crystal size, mm	$0.24 \times 0.24 \times 0.10$
Data scan type	θ–2θ
Scan width, °	$(2.4 + \Delta 2\theta)$
2θ scan range, °	2–30
No. reflections measured	1975
No. unique reflections	1874
R_{int}	0.034
Refinement on F^2	
w$R(F^2)$, all reflections	0.13
$R(F)$, all reflections	0.039
Extinction coefficient	0.0022(3) (Ref. 9)
$\Delta\rho_{max}$, e Å^{-3}	1.46
$\Delta\rho_{min}$, e Å^{-3}	−1.73

RESULTS AND DISCUSSION

The refined atomic coordinates and equivalent isotropic displacement parameters are reported in Table 2. The anisotropic displacement parameters are given in Table 3. Selected interatomic distances and angles are presented in Table 4.

From the structure refinement, the unit cell composition was established to be $Cs_8Ti_4Si_{24}O_{60}$, i.e. $4 \times Cs_2TiSi_6O_{15}$. The calculated analyses for this composition are 36.8 wt% Cs, 23.3 wt% Si, and 6.6 wt% Ti. The cesium and silicon analyses are within the range of measured microprobe values but the titanium is lower than the measured range of 7.2–8.7% Ti. There was no evidence of other partially occupied sites in the final difference Fourier map that could be occupied by excess titanium. A possible explanation is that minor substitution of silicon by titanium occurs, as found for $CsTiSi_2O_{6.5}$ (6), although the Si–O bond lengths listed in Table 4 show no evidence for this. They are, if anything, on the low side for Si–O. Repeat microprobe analyses using different standards for titanium ($CaTiSiO_5$ and $BaTiSi_3O_9$) showed small but consistent variations in the titanium analyses as a function of the standard used and so some doubt is cast on the accuracy of the microprobe results for titanium.

The structure building units are a titanium-centered octahedron, a Si_2O_7 group containing Si(1) and two further silicon-centered tetrahedra containing Si(2) and Si(3). The polyhedra are connected by corner-sharing of all vertices to form an open framework. There are only Ti–O–Si and

TABLE 2
Fractional Atomic Coordinates and Equivalent Isotropic Displacement Parameters (Å^2)

Atom	x	y	z	U_{eq}
Cs	0.11728(3)	0.25839(5)	0.40996(3)	0.0330(2)
Ti	1/4	1/4	0	0.0143(3)
Si(1)	0.0028(1)	0.2682(2)	0.6466(1)	0.0141(3)
Si(2)	0.1554(1)	0.0399(2)	0.1446(1)	0.0231(3)
Si(3)	0.1752(1)	0.4287(2)	0.1663(1)	0.0229(3)
O(1)	0.1189(3)	0.2353(6)	0.1722(3)	0.034(1)
O(2)	0.1973(3)	0.0526(5)	0.0568(2)	0.0233(7)
O(3)	0	0.254(1)	3/4	0.079(4)
O(4)	0.3915(3)	0.1910(7)	0.0750(3)	0.0324(8)
O(5)	0.4483(3)	0.4167(8)	0.3768(4)	0.059(2)
O(6)	0.2531(3)	0.4604(9)	0.2686(3)	0.051(1)
O(7)	0.2359(3)	0.4231(5)	0.0914(3)	0.0311(8)
O(8)	0.4169(4)	0.0732(9)	0.3576(5)	0.079(2)

TABLE 3
Anisotropic Displacement Parameters (Å²)

Atom	U_{11}	U_{22}	U_{33}	U_{23}	U_{13}	U_{12}
Cs	0.0179(2)	0.0341(3)	0.0417(3)	0.0100(1)	0.0011(2)	− 0.0001(1)
Ti	0.0142(5)	0.0177(5)	0.0110(4)	− 0.0038(3)	0.0036(4)	0.0008(3)
Si(1)	0.0106(5)	0.0181(5)	0.0135(5)	0.0013(4)	0.0033(4)	− 0.0039(4)
Si(2)	0.0130(5)	0.0390(8)	0.0151(5)	0.0063(5)	0.0011(4)	0.0001(3)
Si(3)	0.0134(5)	0.0365(7)	0.0159(5)	− 0.0126(5)	0.0003(4)	0.0075(5)
O(1)	0.022(2)	0.056(3)	0.029(2)	− 0.008(2)	0.015(2)	− 0.004(2)
O(2)	0.031(2)	0.022(2)	0.016(1)	− 0.002(1)	0.007(1)	− 0.003(1)
O(3)	0.048(5)	0.17(1)	0.026(4)	0	0.014(4)	0
O(4)	0.017(2)	0.043(2)	0.030(2)	0.005(2)	− 0.003(1)	0.001(1)
O(5)	0.022(2)	0.066(3)	0.073(3)	− 0.041(3)	− 0.008(2)	0.015(2)
O(6)	0.028(2)	0.101(4)	0.019(2)	− 0.016(2)	− 0.002(2)	− 0.013(2)
O(7)	0.047(2)	0.024(2)	0.027(2)	− 0.009(1)	0.019(2)	− 0.002(2)
O(8)	0.037(3)	0.072(4)	0.099(5)	0.057(4)	− 0.022(3)	− 0.034(3)

Si–O–Si linkages between polyhedra. The TiO_6 octahedra are indirectly linked to one another via two intervening SiO_4 tetrahedra. The polyhedral linkages create large cages in which the cesium ions reside. The cages are formed by a three-ring, three 5-rings, two 6-rings, and two 8-rings.

TABLE 4
Selected Interatomic Distances (Å) and Angles (°)

Ti–O(7) (×2)	1.939(3)	180	91.2(2)	93.3(2)
			88.8(2)	86.7(2)
Ti–O(4) (×2)	1.939(4)	91.2(2)	180	90.4(2)
		88.8(2)		89.6(2)
Ti–O(2) (×2)	1.938(3)	93.3(2)	90.4(2)	180
		86.7(3)	89.6(2)	
		O(7)	O(4)	O(2)
Si(1)–O(3)	1.580(1)			
Si(1)–O(4)	1.582(4)	112.9(2)		
Si(1)–O(5)	1.605(5)	107.2(4)	111.9(2)	
Si(1)–O(8)	1.609(5)	107.9(4)	109.5(3)	107.2(4)
		O(3)	O(4)	O(5)
Si(2)–O(2)	1.594(4)			
Si(2)–O(6)	1.610(4)	109.2(2)		
Si(2)–O(5)	1.613(5)	111.4(3)	110.5(3)	
Si(2)–O(1)	1.625(4)	111.8(2)	109.3(3)	104.5(3)
		O(2)	O(6)	O(5)
Si(3)–O(8)	1.589(5)			
Si(3)–O(7)	1.583(4)	112.7(4)		
Si(3)–O(6)	1.600(4)	110.7(3)	111.8(2)	
Si(3)–O(1)	1.638(5)	105.4(3)	111.2(2)	105.4(3)
		O(8)	O(7)	O(6)
Cs–O(1)	3.030(5)	Cs–O(5)	3.336(6)	
Cs–O(2)	3.156(3)	Cs–O(8)	3.459(7)	
Cs–O(7)	3.173(4)	Cs–O(6)	3.536(5)	
Cs–O(4)	3.224(5)	Cs–O(7)	3.607(4)	
Cs–O(2)	3.232(4)	Cs–O(1)	3.608(4)	

A polyhedral representation of the structure, viewed down the unique axis, *b*, is given in Fig. 1. This view shows clearly the 5-rings and 6-rings. The former involves the edges of a TiO_6 octahedron, a $Si(1)_2O_7$ group and two SiO_4 tetrahedra, while the latter includes an additional octahedral edge. A second type of 5-ring, which is perpendicular to the section shown in Fig. 1, involves the edges of five tetrahedra. It is seen from Fig. 1 that parallel to (001), narrow blocks containing only TiO_6 octahedra are separated by blocks containing zigzag chains of Si_2O_7 groups. The Si_2O_7 groups are oriented approximately along [101] and [001] in the chains. These chains are linked along [010]

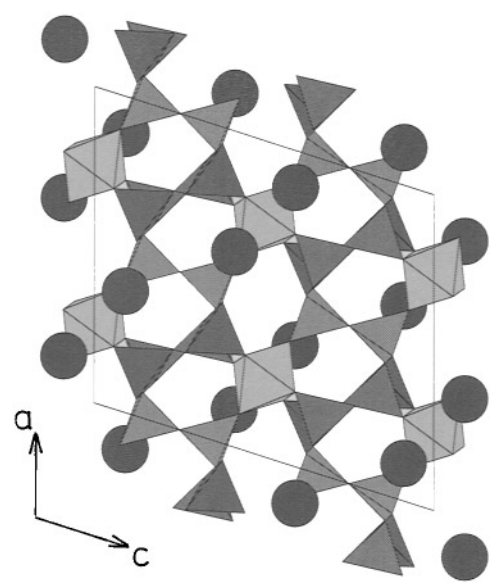

FIG. 1. Polyhedral representation of the structure of $Cs_2TiSi_6O_{15}$, projected along the *b* axis. Filled circles represent cesium ions. $Si(1)O_4$ to $Si(3)O_4$ tetrahedra are distinguished by increasing density of shading.

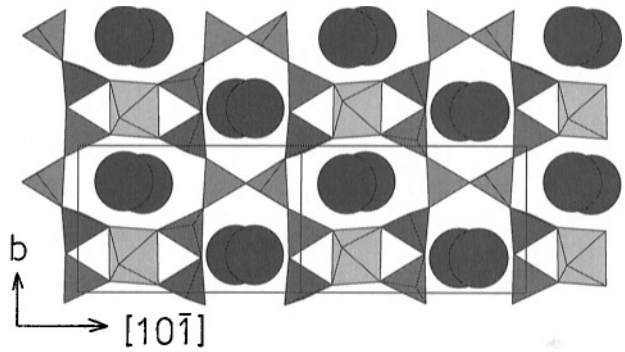

FIG. 2. (101) slice of the structure of $Cs_2TiSi_6O_{15}$, viewed along [101]. Filled circles represent cesium ions on either side of the polyhedral layer. $Si(1)O_4$ to $Si(3)O_4$ tetrahedra are distinguished by increasing density of shading.

by further corner sharing into blocks parallel to (001). This plane is the main growth plane of the platy or tabular crystals.

From Fig. 1 it is seen that the cesium ions form undulating rows, oriented along [101]. Alternately short and long Cs–Cs separations occur along the rows with distances of 3.765(2) and 4.904(2) Å. The next shortest Cs–Cs separation is 5.946(2) Å, between cesium ions in adjacent [101] rows. Figure 2 shows a view of the structure parallel to the [101] rows of cesium ions. It is seen that the cavities containing the cesium ions have large apertures normal to this direction, formed from 8-rings of two types. One is formed from the edges of eight tetrahedra (8T) while the other is formed from the edges of six tetrahedra and two octahedra (6T + 2O). Both apertures are compressed into elliptical shapes. The principal axes of the two types of ellipses are orthogonal. The cavities containing cesium ions are connected via these apertures into channels parallel to [101]. The minimum free diameter of the 6T + 2O aperture is about 2.5×4.8 Å, based on an O radius of 1.35 Å. The corresponding value for the 8T aperture is 1.8×4.2 Å. However, this aperture is constricted at the center and is probably better described as comprising two adjacent minimum free diameters, each about 2.1×2.1 Å. It is clear that the cesium ions, with a diameter of at least 3.5 Å, will not be free to migrate along the channels.

Ball-and-stick models of the two types of 8-ring apertures are presented in Fig. 3, showing the anisotropic displacement ellipsoids. Whereas the oxygen atoms forming the TiO_6 octahedra, O(2), O(4), and O(7), show only moderate anisotropy, the oxygens involved in Si–O–Si linkages are highly anisotropic, particularly those associated with the $Si(1)_2O_7$ group, O(3), O(5), and O(8). The principal displacement axes for these oxygens are almost in the plane of projection in Fig. 3. The orientation of the ellipsoids is suggestive of cooperative rotation of the Si(1)-centered tetrahedra about the apical Si(1)–O(4) bonds that form the Si–O–Ti linkages.

The short Cs–Cs interatomic distance of 3.76 Å occurs across the 8-ring aperture shown in Fig. 3a, comprising six tetrahedra and two octahedra. The cesium cations are

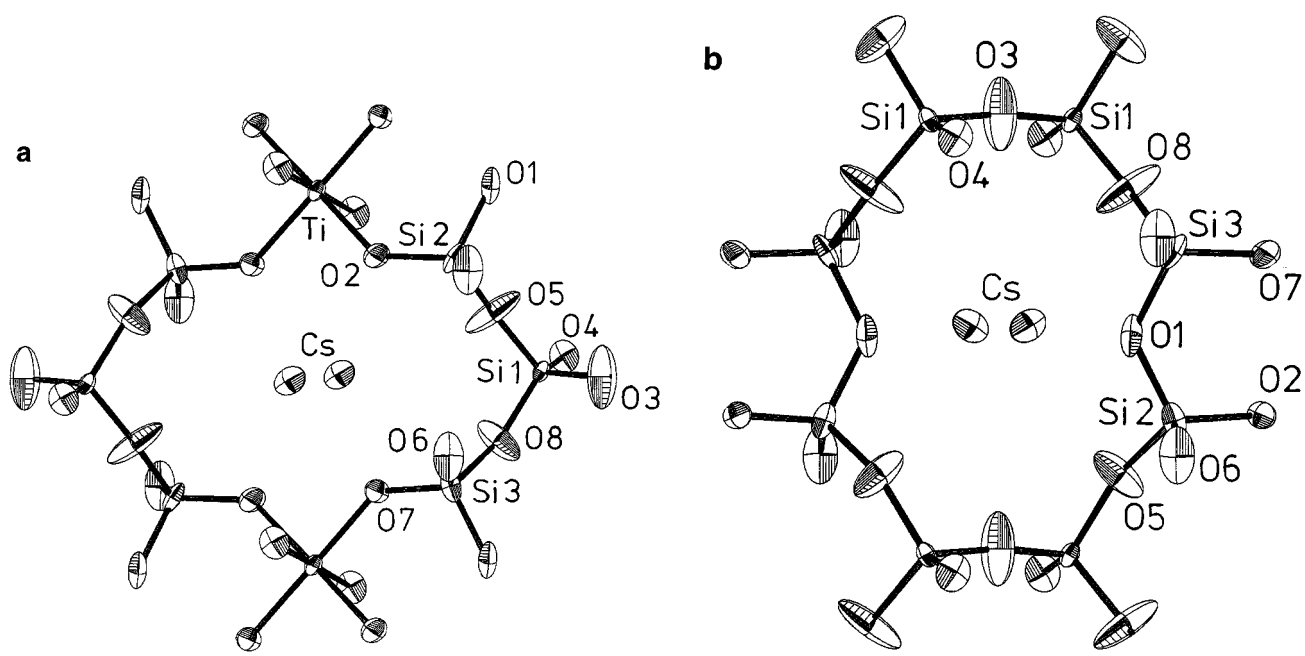

FIG. 3. Atom connectivity in the 8-membered rings formed by (a) six tetrahedra and two octahedra and (b) eight tetrahedra. Anisotropic displacement ellipsoids (50% probability) are shown.

shielded in the plane of the aperture by the rectangle of four oxygens, $2 \times [O(2) + O(7)]$, which form the two octahedral edges. It is interesting to note that in the cesium hollandite phase, $Cs_{1.36}Ti_8O_{16}$, pairs of cesium ions along the hollandite tunnels are also shielded by four oxygens, and the Cs–Cs separation of 3.72 Å (10) is very close to the short Cs–Cs distance in $Cs_2TiSi_6O_{15}$. In the cesium hollandite the four oxygens form a square planar arrangement rather than a rectangle, but the cross-section area defined by the four anion positions is about the same in both compounds. in $Cs_2TiSi_6O_{15}$, the longer Cs–Cs separation of 4.90 Å occurs across the 8-ring aperture comprising 8 tetrahedral edges. As seen in Fig. 3b the main shielding of the cesium cations is by only two oxygens in this case. The short Cs–Cs distances of 3.72 Å in cesium hollandite and 3.76 Å in $Cs_2TiSi_6O_{15}$ are to be compared to a separation between cesium atoms in the bcc metal of 5.25 Å (11).

The interatomic distances and angles for the framework polyhedra are given in Table 4. The TiO_6 octahedron shows only slight departurres from ideal geometry. The three independent Ti–O distances are identical at 1.939(4) Å and the O–Ti–O angles range from 86.7(2) to 93.3(2)°. The mean Ti–O distance is identical to that in benitoite, $BaTiSi_3O_9$, which also possesses a framework of isolated TiO_6 octahedra sharing all corners with SiO_4 tetrahedra (12). The three SiO_4 tetrahedra are also quite regular, with Si–O distances in the range 1.580(1) to 1.638(5) Å and O–Si–O angles in the range 104.5(3) to 112.9(2)°. The average Si(1)–O, Si(2)–O and Si(3)–O distances are 1.594, 1.610, and 1.603 Å. The latter two distances agree with reported mean Si–O distances in zeolites with ordering of silicon and aluminium (13, 14). The shorter mean Si(1)–O distance involves those oxygens that have the largest anisotropic displacement parameters, so the actual Si–O distances will be longer than obtained in the refinement. The cesium ion has 10 closest oxygen neighbors, with Cs–O distances in the range 3.030(5) to 3.608(4) Å and a mean Cs–O value of 3.336 Å. This is of the order of 0.2 Å longer than the mean Cs–O distance in cesium hollandite where the cesium is eight-coordinated (10), but shorter than the mean Cs–O distance of 3.48 Å in pollucite (15), in which the cesium is twelve coordinated.

COMPARISON WITH OTHER STRUCTURES

The structure of $Cs_2TiSi_6O_{15}$ represents a new type of microporous titanosilicate framework structure. The ordering of titanium atoms into isolated, undistorted octahedra so that there are only Si–O–Si and Ti–O–Si linkages in the framework is relatively unusual. This situation also occurs in the mineral benitoite, $BaTiSi_3O_9$ (12). However reported titanosilicates containing TiO_6 octahedra generally have higher Ti/Si ratios and involve Ti–O–Ti linkages, which form octahedral clusters as in $Na_2Ti_2O_3SiO_4 \cdot 2H_2O$ (16) and $Cs_3HTi_4O_4(SiO_4)_3 \cdot 4H_2O$ (17) or linear chains as in ETS-10 (Engelhard Corporation titanosilicate) (18).

The other known cesium titanosilicate structure is that of $CsTiSi_2O_{6.5}$ (6), which differs significantly from that for $Cs_2TiSi_6O_{15}$ in having the titanium atoms disordered over the tetrahedral sites in a pollucite type framework. Relative to pollucite, $CsAlSi_2O_6$, there are extra oxygen atoms in the unit cell and Ti-EXAFS studies indicate that these are coordinated to titanium so that the tetrahedral coordination is modified locally to 5-coordination (6). Five coordinated titanium occurs in layered titanosilicates such as the mineral fresnoite, $Ba_2TiSi_2O_8$ (19) and $Na_4Ti_2Si_8O_{22} \cdot 4H_2O$ (20). In these compounds the titanium has square pyramidal coordination with a very short apical bond typical of the titanyl group.

Work in progress indicates that $Cs_2TiSi_6O_{15}$ has a high durability towards leaching. It thus has potential for containment of cesium selectively adsorbed onto titanosilicate ion exchangers from sodium-rich radioactive wastes.

ACKNOWLEDGMENTS

We appreciate help from Terrell Vanderah (NIST) with the crystal growth and from Colin McRae with the microprobe analyses. We thank Larry Henling of CalTech and Lachlan Cranswick for checking the structure model using direct methods.

REFERENCES

1. S. M. Kuznicki, U.S. Patent 4567029 (1989).
2. D. M. Chapman and A. L. Roe, *Zeolites* **10,** 730 (1990).
3. M. Taramasso, G. Perego, and B. Notari, U.S. Patent 4410501 (1983).
4. R. G. Anthony, C. V. Phillip, and R. G. Dosch, *Waste Management* **13,** 503 (1993).
5. M. L. Balmer and B. C. Bunker, "Inorganic Ion Exchange Evaluation and Design—Silicotitanate Waste Form Conversion," PNL-10460, March 1995.
6. M. L. Balmer, Q. Huang, W. Wong-Ng, R. S. Roth, and A. Santoro, submitted for *J. Solid State Chemistry*
7. K. Yanagisawa, M. Nishioka, and N. Yamasaki, *J. Nucl. Sci. Technol.* **24,** 51 (1987).
8. G. M. Sheldrick, "SHELX 76, Program for Crystal Structure Determination," Univ. of Cambridge, Cambridge, UK, 1976.
9. G. M. Sheldrick, "SHELXL93, Program for the Refinement of Crystal Structures," Univ. Göttingen, Göttingen, 1993.
10. R. W. Cheary, *Acta Crystallogr. Sect. B* **47,** 325 (1991).
11. C. S. Barrett, *Acta Crystallogr.* **9,** 671 (1956).
12. K. Fischer, *Z. Kristallogr.* **129,** 222 (1969).
13. E. Galli, *Acta Crystallogr. Sect. B* **32,** 1623 (1976).
14. I. S. Kerr and D. J. Williams, *Acta Crystallogr. Sect B* **25,** 1183 (1969).
15. R. E. Newnham, *Am. Mineral.* **52,** 1515 (1967).
16. D. M. Poojary, R. A. Cahill, and A. Clearfield, *Chem. Mater.* **6,** 2364 (1994).
17. W. T. Harrison, T. E. Gier, E. Thurman, and G. D. Stucky, *Zeolites* **15,** 408 (1995).
18. M. W. Anderson, O. Terasaki, T. Ohsuna, A. Philippou, S. P. MacKay, A. Ferreira, J. Rocha, and S. Lidin, *Nature* **367,** 347 (1994).
19. S. A. Markgraf, A. Halliyal, A. S. Bhalla, R. E. Newnham, and C. T. Prewitt, *Ferroelectrics* **62,** 17 (1985).
20. M. A. Roberts, G. Sankar, J. M. Thomas, R. H. Jones, H. Du, J. Chen, W. Pang, and R. Xu, *Nature* **381,** 401 (1996).